NJC

New Journal of Chemistry

A journal for new directions in chemistry

Accepted Manuscript

This article can be cited before page numbers have been issued, to do this please use: H. L. T. Mai, N. T. T. Truong, Q. Nguyen, B. K. Doan, D. H. Tran, L. T. Nguyen, W. Lee, J. W. Jung, H. M. Hoang, H. K. P. Ha, C. D. Tran and H. Tran Nguyen, *New J. Chem.*, 2020, DOI: 10.1039/D0NJ02616F.

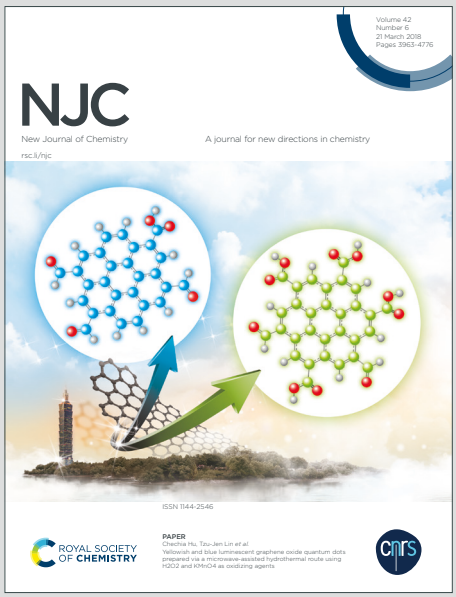

This is an Accepted Manuscript, which has been through the Royal Society of Chemistry peer review process and has been accepted for publication.

Accepted Manuscripts are published online shortly after acceptance, before technical editing, formatting and proof reading. Using this free service, authors can make their results available to the community, in citable form, before we publish the edited article. We will replace this Accepted Manuscript with the edited and formatted Advance Article as soon as it is available.

You can find more information about Accepted Manuscripts in the Information for Authors.

Please note that technical editing may introduce minor changes to the text and/or graphics, which may alter content. The journal's standard Terms & Conditions and the Ethical guidelines still apply. In no event shall the Royal Society of Chemistry be held responsible for any errors or omissions in this Accepted Manuscript or any consequences arising from the use of any information it contains.

View Article Online
DOI: 10.1039/D0NJ02616F

View Article Online
DOI: 10.1039/D0NJ02616F

Synthesis and Characterization of Donor-Acceptor Semiconducting Polymers Containing 4-(4-((2-ethylhexyl)oxy)phenyl)-4H-dithieno[3,2-b:2',3'-d]pyrrole for Organic Solar Cells

Huyen Le Thi Mai[1], Nhung Thanh Thi Truong[1,2], Thiet Quoc Nguyen[3], Bao Kim Doan[1], Dat Hung Tran[1], Le-Thu T.Nguyen[2], Lee Woosung[4], Jae Woong Jung[5], Mai Ha Hoang[6], Ha Phuong Ky Huynh[2], Chau Duc Tran*[2], Ha Tran Nguyen*[1,2]

[1]National Key Laboratory of Polymer and Composite Materials, Ho Chi Minh City University of Technology, Vietnam National University–Ho Chi Minh City (VNU–HCM), 268 Ly Thuong Kiet, District 10, Ho Chi Minh City, Vietnam.

[2]Faculty of Materials Technology, Ho Chi Minh City University of Technology (HCMUT), Vietnam National University, 268 Ly Thuong Kiet, District 10, Ho Chi Minh City, Vietnam

[3] Institute of Applied Materials Science, Vietnam Academy of Science and Technology, 01 TL29, District 12, Ho Chi Minh City, Vietnam

[4] Smart textile R&D group, Korea Institute of Industrial Technology, Ansan, (KITECH)

[5] Department of Advanced Materials Engineering for Information & Electronics, Kyung Hee University, 1732 Deogyeong-daero, Giheung-gu, Yongin-si, Gyeonggi-do 446-701, Republic of Korea

[6] Institute of Chemistry, Vietnam Academy of Science and Technology, Hanoi, Vietnam

** Corresponding author. Email address: nguyentranha@hcmut.edu.vn*

Abstract

In this study, new donor-acceptor (D-A) conjugated polymers based on 4-(4-((2-ethylhexyl)oxy)phenyl)-4H-dithieno[3,2-b:2',3'-d]pyrrole (EPDP) and 3,6-bis(5-bromothiophen-2-yl)-2,5-bis(2-ethylhexyl)-2,5-dihydropyrrolo[3,4-c]pyrrole-1,4-dione (BTBP) or 4,7-bis(5-bromothiophen-2-yl)benzo[c][1,2,5]thiadiazole (BT) have been synthesized successfully via direct(hetero)arylation polymerization using $Pd(OAc)_2$ and $PCy_3.HBF_4$ as catalyst system. The obtained D-A conjugated polymers have been characterized via ^1H NMR, GPC, FTIR, DSC, XRD, PL and UV-Vis methods. Afterward, the D-A conjugated polymers have been applied for the fabrication of organic solar cells based on bulk-heterojunction (BHJ) structures.

Key words: *Donor-acceptor (D-A) conjugated polymers, Direct Arylation Polymerization, Organic Solar Cells, Bulk heterojunction structure, Dithieno [3,2-b:2',3'-d]pyrrole*

View Article Online
DOI: 10.1039/D0NJ02616F

1. Introduction

Today, organic solar cells (OSCs) have emerged as potential candidates as renewable energy resources because of their tremendous advantages.[1-7] The power conversion efficiencies (PCEs) of OSCs have enhanced up to 18% where conjugated copolymers as donor moieties combined with fullerene/non-fullerene derivatives as acceptors were applied in bulk-heterojunction structures.[8-17] Among novel conjugated polymers, the type of alternating donor–acceptor (D-A) conjugated copolymers containing both electron donor and electron acceptor segments has exhibited extremely narrow bandgaps, red-shifts in absorption wavelength and excellent thermal stability. However, one of the main challenges in organic photovoltaics is the loss of energy in photon absorption process and the optimal balance between the PCEs and open-circuit voltage (V_{oc}) which influences the gap between HOMO and LUMO levels in donor and acceptor materials.[18] Hence, selecting appropriate donor and acceptor units in D-A materials plays a key role in handling these issues. Recently, conjugated polymers based on dithieno[3,2-b:2,3-d]pyrroles (DTPs) have showed favorable results, including reduced band gaps, high carrier mobilities, and the stability in the oxidized state owing to the electron-rich N atom in their structure.[19,20]

Among strong electron–withdrawing units, benzothiadiazole (BT) and diketopyrrolopyrrole (DPP) have been used efficiently in D-A conjugated polymers for OSC and organic field-effect transistor (OFET) devices because of their planar and electron withdrawing structures.[1,4,6] In 2013, Dou *et. al* reported the charge transport properties of a low band gap conjugated polymer named PBDTT-Se-DPP, which exhibited a PCE of 7.2% (E_g= 1.38 eV; J_{SC} = 16.8 mA/cm^{-2}; V_{OC}= 0.69 V).[21] In 2014, Ashraf *et. al* reported the polymer PDPP2TT-T with PCE up to 8% (E_g= 1.39 eV; J_{SC}= 23.5 mA/cm^{-2}; V_{OC} = 0.57 V).[22] Following this achievement, PDPP2TT-TT has been synthesized and explored with PCE reaching to 9.4% (E_g= 1.35 eV; J_{SC} = 20.1 mA/cm^{-2}; V_{OC}= 0.67 V) in 2015.[23] On the other hand, BT unit is also a favorable electron-drawing with good π-π stacking, strong intermolecular interactions and simple synthesis procedure.[24] In 2019, Chen *et. al* reported the polymers PE2: BTA3 and PE1: BTA3 with PCE of 5.83% (J_{SC}= 8.06 mA/cm^{-2}; V_{OC} = 1.26 V) and 8.43 % (J_{SC}= 11.95 mA/cm^{-2}; V_{OC} = 1.11 V), respectively.[25] The photovoltaic polymer PDPP2TzDTP based on DTP and BT was studied by Li *et al.* with a PCE of 5.6% (E_g= 1.67 eV; J_{SC} = 14.9 mA/cm^{-2}; V_{OC} = 0.69 V) in 2015 [10]. Geng *et al.* also reported the conjugated polymer PDTP-DT2BT with a PCE of 3.12% (E_g= 1.59 eV; J_{SC} = 11.43 mA/cm^{-2}; V_{OC} = 0.31 V, PCE = 3.12 %).[26] Nagarjuna *et. al* reported OSCs based on PTB7-Th polymer in combination with $PC_{70}BM$ and modified $PC_{70}BM$ (CN-$PC_{70}BM$), with PCEs of 5.4% and 8.2%, respectively.[27] Wan *et. al* also reported PTB7-Th:CN-PC70BM based OSCs with the structure of ITO/PEDOT:PSS/PTB7-Th: $PC_{61}BM$ (1:1.5, w/w)/C60 –N (16 nm)/Al, giving a PCE of 10.8% in the presence of 1.5% DIO + 1.5% NMP additives, whereas without additives only a PCE of 8.1% was obtained.[28] This result suggested that the modification

View Article Online
DOI: 10.1039/D0NJ02616F

of acceptor moieties of PCBM and binary additives have an important role for incorporating donor and acceptor units for charge transport properties. On the other hand, conjugated polymers based on DTP moieties exhibit HOMO levels closed to that of $PC_{60}BM$ acceptor units as well as good stability in the oxidized state, which could be more promising for OSCs in comparison with PTB7-Th copolymer systems. However, there have not been any reports related to the synthesis and characterization of conjugated polymers based on DPP and 4,7-bis(5-bromothiophen-2-yl)benzo[c][1,2,5]thiadiazole with 4-(4-((2-ethylhexyl)oxy)phenyl)-4H-dithieno[3,2-b:2',3'-d]pyrrole.

Therefore, in this research, the alternating D-A conjugated polymers poly[4-(4-((2-ethylhexyl)oxy)phenyl)-4H-dithieno[3,2-b:2',3'-d]pyrrole-*alt*-3,6-bis(5-bromothiophen-2-yl)-2,5-bis(2-ethylhexyl)-pyrrolo[3,4-c]pyrrole-1,4(2H)-dione] (P1) and Poly[4-(4-((2-ethylhexyl)oxy)phenyl)-4H-dithieno[3,2-b:2',3'-d]pyrrole-*alt*-4,7-bis(5-bromothiophen-2-yl)benzo[c][1,2,5]thiadiazole] (P2) have been designed and synthesized via direct (hetero)arylation polymerization using palladium(II) acetate ($Pd(OAc)_2$) and tricyclohexylphosphine tetrafluoroborate ($PCy_3.HBF_4$) as catalyst and ligand, respectively. The obtained novel conjugated polymers have been characterized via ^1H NMR, FT–IR, XRD, UV-Vis and photoluminescence (PL) spectroscopies as well as thermal analysis including differential scanning calorimetry (DSC) and thermogravimetric analysis (TGA). Additionally, the organic solar cells based on these conjugated polymers have been fabricated and their PCEs have been evaluated.

2. Experimental Section

2.1. Materials

2-ethylhexyl bromide (95%), palladium(II) acetate ($Pd(OAc)_2$, 98%), tricyclohexylphosphine tetrafluoroborate ($PCy_3{\cdot}HBF_4$, 97%), 3,3′dibromo-2,2′bithiophene, benzamide, N,N′-dimethylethylenediamine (DMEDA, 85%) and pivalic acid (PivOH, 99%), tri(tert-butyl)phosphine (P(t-Bu)$_3$ were purchased from Sigma-Aldrich/Kantochem and used as received. 4-Iodine phenol (99%), potassium carbonate (K_2CO_3, 99%), sodium *tert*-butoxide (NaOt-Bu, 98%), magnesium sulfate ($MgSO_4$, 98%), and copper iodine (CuI, 99.9%) were purchased from Acros/Merck. Chloroform ($CHCl_3$, 99.5%), dichloromethane (CH_2Cl_2, 99.5%), toluene (99.5%), acetonitrile (CH_3CN, 99.8%) and dimethylacetamide (DMAc, 99%) were purchased from Fisher/Acros/Sigma as well as dried using molecular sieves under N_2. Acetone (99.6%), n-heptane (99%), methanol (99.8%) and ethyl acetate (99%) were purchased from Fisher/Acros and used as received.

2.2. Measurements

View Article Online
DOI: 10.1039/D0NJ02616F

^{1}H NMR spectra were recorded in deuterated chloroform ($CDCl_3$) with tetramethylsilane (TMS) as an internal reference, on a Bruker Avance 500 MHz. Fourier transform infrared (FT-IR) spectra, collected as the average of 264 scans with a resolution of 4 cm^{-1}, were recorded from a KBr disk on the FTIR Bruker Tensor 27. Size exclusion chromatography (SEC) measurements were performed on a Polymer PL-GPC 50 gel permeation chromatography (GPC) system equipped with an RI detector, with chloroform ($CHCl_3$) and tetrahydrofuran (THF) as the eluent at a flow rate of 1.0 mL min^{-1}. Molecular weights and molecular weight distributions were calculated with reference to polystyrene standards. Elemental analyses were performed by the Dumas combustion method, using a Costech ECS 4010 Elemental Analyzer

UV–visible absorption spectra of all polymers in solution and polymer thin films were recorded on a Shimadzu UV-2450 spectrometer over the wavelength range 300–900nm. Fluorescence spectra (PL) were measured on a Horiba IHR 325 spectrometer.

Differential scanning calorimetry (DSC) measurements were carried out with a DSC 204 F1— NETZSCH instruments under nitrogen flow (heating rate 10 °C min^{-1}). Thermogravimetric analysis (TGA) measurements were performed under nitrogen flow using a STA 409 PC Instruments with a heating rate of 10°C min^{-1} from ambient temperature to 1000°C.

Wide-angle powder XRD patterns were recorded at room temperature on a Bruker AXS D8 Advance diffractometer using Cu-K_α radiation (k = 0.15406 nm), at a scanning rate of 0.05°s^{-1}. The data were analyzed using DIFRAC plus Evaluation Package (EVA) software. The *d*-spacing was calculated from peak positions using Cu-K_α radiation and Bragg's law. Atomic force microscopy (AFM) images were obtained using a Bruker Dimension 3100 atomic force microscope. Elemental analyses were performed by the Dumas combustion method, using a Costech ECS 4010 elemental analyzer.

Electrochemical measurements were performed on an AUTOLAB machine (software NOVA 1.11) using an Au disc working electrode and a Pt wire counter electrode. Solutions consisted of 0.1 M TBAPF6 in CH_3CN and were purged with argon for 20 min prior to data collection. All potentials are referenced to a Ag/Ag+ reference electrode (0.1 M $AgNO_3$/0.1 M TBAPF6 in CH_3CN; 0.320 V vs. SCE) and internally standardized with ferrocene (vs. Ag/Ag+). E_{HOMO} values were determined in reference to ferrocene. The polymer film was coated on electrode washed with CH_3CN and placed in a cell with a fresh electrolyte solution for electrochemical characterization.

View Article Online
DOI: 10.1039/D0NJ02616F

The current density–voltage (*J–V*) characteristic curves were recorded in a computer-controlled Keithley 2400 source unit. Solar cell performance was measured using Air Mass 1.5 Global (AM 1.5G) under a simulated solar irradiance.

2.3. Synthesis of 1-((2-ethylhexyl)oxy)-4-iodobenzene (compound 3) (M1)

4-Iodine phenol (1000 mg, 4.55 mmol) (compound 1), 2-ethylhexyl bromide (1757 mg, 9.09 mmol) (compound 2), K_2CO_3 (1258 mg, 9.10 mmol) were dissolved in acetonitrile (10 ml) in a 100 ml flask. Then, the mixture was stirred and heated at 82 °C for 48 h under nitrogen atmosphere. After finishing and cooling down to room temperature, the compound was extracted in $CHCl_3$, washed with distilled water, dried over anhydrous K_2CO_3, filtered and vacuum-evaporated to remove the solvent. The crude product was purified by silica column chromatography using n-hexane as the eluent and dried under vacuum at 50 °C in 24 h in order to obtain the isolated product as a light yellow oil (2.09 g, R_f= 0.7, yield: 97%).

^{1}H NMR (500 MHz, $CDCl_3$), δ (ppm): 7.52 (d, 2H), 6.68 (d, 2H), 3.80 (m, 2H), 1.7 (m, 1H), 1.33-1.44 (m, 8H), 0.91 (m, 6H). Analysis calculated for $C_{14}H_{21}IO$: C, 50.61; H, 6.37; I, 38.20; O, 4.82. Found: C, 49.21; H, 6.15; I, 38.3; O, 6.34.

2.4. Synthesis of 4H-dithieno[3,2-b:2′,3′-d]pyrrole (compound 6) (M2)

The synthesis of the compound 4H-dithieno[3,2-b:2′,3′-d]pyrrole (M2) was carried out by the previously reported procedure.[29] A flame-dried Schlenk two-neck round-bottom flask with a magnetic stir bar is charged with toluene and H_2O. The solvent was degassed through freeze-pump-thaw cycle for 3 times. Then DMEDA (423.12 mg; 4.8 mmol) and CuI (228.54 mg; 1.2 mmol) were added to the flask under N_2 atmosphere, followed by stirring for several minutes. Benzamide (872.21 mg; 7.2 mmol), 3,3'-Br_2-2,2'-bithiophene (1944.3 mg; 6 mmol) and K_2CO_3 (2487.78 mg; 18 mmol) were added and the mixture was degassed via freeze-pump-thaw cycle for three times. In the following stage, the reaction was heated at 110 °C for 48 h. Afterward, the reaction was cooled to room temperature, quenched with H_2O and extracted with dichloromethane. The organic layer was washed with NaCl solution and distilled water then dried over K_2CO_3. The mixture was filtered and concentrated via rotary evaporation. The crude product was purified by silica gel chromatography using ethyl acetate/n-hexane = 1:15 (v/v) and dried under vacuum at 50 °C in 24 h to obtain the pure compound as a white crystalline solid (630 mg, R_f= 0.17, yield: 58.57%).

^{1}H NMR (500 MHz, $CDCl_3$), δ (ppm): 8.31 (s, 1H), 7.02 (d, 2H), 7.14 (d, 2H). Analysis calculated for $C_8H_5NS_2$: C, 53.60; H, 2.81; N, 7.81; S, 35.77. Found: C, 54.10; H, 2.67; N, 7.85; S, 35.38.

View Article Online
DOI: 10.1039/D0NJ02616F

2.5. Synthesis of 4-(4-((2-ethylhexyl)oxy)phenyl)-4H-dithieno[3,2-b:2',3'-d]pyrrole (compound 7) (M3)

In a two-neck flask connected with a Schlenk line, $Pd(OAc)_2$ (2.51 mg; 0.023 mmol), $P(t\text{-}Bu)_3$ (4.52 mg; 0.058 mmol) and toluene (5 ml) were added and stirred at the room temperature for 10 min. In the next step, **(M1)** (139 mg; 0.846 mmol), **(M2)** (50 mg; 0.564 mmol) and NaOt-Bu (80.44 mg; 1.692 mmol) were added. The mixture reaction was bubbled with nitrogen for 30 min and then stirred at 110 °C for 24 h. After cooling to ambient temperature, the mixture was extracted with dichloromethane, washed with NaCl solution and distilled water as well as dried over K_2CO_3, filtered, concentrated via rotary evaporation. The crude product was purified by column chromatography (silica gel) using ethyl acetate/n-hexane = 1:200 (v/v) as eluent and dried under vacuum at 50 °C in 24 h in order to obtain the main product as a green solid (24.2 mg, R_f= 0.45, yield: 22.6%).

^{1}H NMR (500 MHz, $CDCl_3$), δ (ppm): 7.47 (d, 2H), 7.14 (d, 2H), 7.08 (d, 2H), 7.04 (d,2H), 3.89 (d,2H), 1.78 (m, 1H), 1.48-1.34 (m, 8H), 0.96 (m, 6H). Analysis calculated for $C_{22}H_{25}NOS_2$: C, 68.89; H, 6.57; N, 3.65; O, 4.17; S, 16.72. Found: C, 69.2; H, 6.62; N, 3,71; O, 4.07; S, 16.40.

2.6 Synthesis of conjugated polymer Poly[4-(4-((2-ethylhexyl)oxy)phenyl)-4H-dithieno[3,2-b:2',3'-d]pyrrole-*alt*-3,6-bis(5-bromothiophen-2-yl)-2,5-bis(2-ethylhexyl)-pyrrolo[3,4-c]pyrrole-1,4(2H)-dione] (compound 9) (P1)

In a glove box, 4-(4-((2-ethylhexyl)oxy)phenyl)-4H-dithieno[3,2-b:2',3'-d]pyrrole (M3) (50 mg 0.1304 mmol) and 3,6-bis(5-bromothiophen-2-yl)-2,5-bis(2-ethylhexyl)-2,5-dihydropyrrolo[3,4-c]pyrrole-1,4-dione (88.98 mg 0.1304 mmol) were dissolved in 3 ml of DMAc. Subsequently, $Pd(OAc)_2$ (1.46 mg 0.007 mmol), $PCy_3.HBF_4$ (4.8 mg 0.01 mmol), PivOH (13.31 mg 0.1304 mmol) and K_2CO_3 (54.07 mg 0.391 mmol) were added to the monomers' solution. Before being removed from the glove box, the vial was sealed with a rubber cap. Then, the vial was heated in a 100 °C in oil bath for 24 h. After being cooled to room temperature, the reaction mixture was diluted with 30 mL of chloroform. The mixture was precipitated in methanol and purified via Soxhlet extraction with *n*-heptane, acetone and chloroform in order to remove low molecular weight fractions. The resulting polymer was isolated by filtration, washed with acetone and finally dried under reduced pressure at 50 °C for 24 h. A dark blue solid was obtained with a yield of 69%.

^{1}H NMR (500 MHz, $CDCl_3$), δ (ppm): 8.50 – 9.25 (m, 2H), 6.61 – 7.61 (m, 8H), 4.00 (d, 4H), 0.7 – 1.95 (m, 45H). GPC: M_n = 12.700 g/mol. Đ (M_w/M_n) = 1.87. Analysis calculated for $[C_{52}H_{63}O_3N_3S_4]_{14}$ found: C, 67.81; H, 8.01; N, 4.94; S, 13.76.

View Article Online
DOI: 10.1039/D0NJ02616F

2.7 Synthesis of conjugated polymer of poly[4-(4-((2-ethylhexyl)oxy)phenyl)-4H-dithieno[3,2-b:2',3'-d]pyrrole-alt-4,7-bis(5-bromothiophen-2-yl)benzo[c][1,2,5]thiadiazole] (compound 11) (P2)

In a glove box, 4-(4-((2-ethylhexyl)oxy)phenyl)-4H-dithieno[3,2-b:2',3'-d]pyrrole (50 mg 0.1304 mmol) and 4,7-bis(5-bromothiophen-2-yl)benzo[c][1,2,5]thiadiazole (59.75 mg 0.1304 mmol) were dissolved in 3 ml of DMAc. Then, $Pd(OAc)_2$ (1.46 mg 0.007 mmol), $PCy_3.HBF_4$ (4.80 mg 0.013 mmol), PivOH (13.31 mg 0.1304 mmol) and K_2CO_3 (54.07 mg 0.3912 mmol) were added to the monomer solution. Before being removed from the glove box, the vial was sealed with a rubber cap. Then, the vial was heated in a 100 °C oil bath for 24 h. After being cooled to room temperature, the reaction mixture was diluted with 30 mL of chloroform. The mixture was precipitated in methanol and purified via Soxhlet extraction with *n*-heptane, acetone and chloroform in order to remove low molecular weights fraction. The resulting polymer was isolated by filtration, washed with acetone and finally dried under reduced pressure at 50 °C for 24 h. A dark purple solid was obtained with yield of 65%.

^{1}H NMR (500 MHz, $CDCl_3$), δ (ppm): 8.07 – 7.53 (m, 6H), 7.09 (m, 4H), 3.96 (s, 2H), 2.69 (s, 2H), 2.81 (s, 2H), 0.8 – 1.98 (m, 37H). GPC: M_n = 14.800 g/mol. Đ (M_w/M_n) = 1.65. Analysis calculated for $[C_{48}H_{55}ON_3S5]_{17}$ found: C, 66.80; H, 6.37; N, 5.01; S, 17.82.

2.8 Solid state film preparation

Solid state polymer thin films were prepared by spin-coating from polymer solutions in chloroform with a concentration of 3 mg/ml and then dried at 70 °C for 60 min.

2.9 Fabrication and characterization of bulk-heterojunction polymer solar cell structure

First, the ITO substrates (10 Ω/sq) were cleaned by ultrasonication with deionized water, acetone and isopropyl alcohol respectively. The devices were fabricated with a bulk-heterojunction (BHJ) structure with an configuration of ITO/PEDOT:PSS/conjugated polymer:$PC_{61}BM$/Ca/Al. The film was annealed at 200 °C for 1 h, and then transferred into a N_2-filled glove box to spin-cast the active layer. The solution containing a mixture of polymer:$PC_{61}BM$ (weight ratio is 1:1.5) in chlorobenzene solvent with 1.0 vol% of 1,8-diiodooctane (DIO). This was then followed by thermal annealing at 100 °C for 5 min. Then, Ca and Al were successively deposited by thermal evaporation in a vacuum less than 1 x 10^{-6} Torr with deposition rate of 0.3 nm s^{-1}.

2.10 Fabrication and characterization of OFETs

The polymers P1 and were applied to fabricate the OFETs on oxidized silicon wafer to determine the charge mobilities of semiconducting polymers. 80 nm thick films of the P1 and P2 conjugated

View Article Online
DOI: 10.1039/D0NJ02616F

polymers were spin-coated on silicon wafer substrates under argon environment, followed by film drying and annealing at 150 °C for 15 min. Finally, OFET devices were completed by evaporating gold source and drain contacts through a shadow mask. The electrical properties of OFETs devices Keithley 4200 semiconductor parameter analyzer equipment was used to characterize the electrical properties of OFETs devices.

3. Results and Discussion

3.1 Synthesis and characterization of monomers and conjugated polymers

The synthetic route for preparation of 1-((2-ethylhexyl)oxy)-4-iodobenzene (Compound 1, M1), 4H-dithieno[3,2-b:2′,3′-d]pyrrole (M2) and 4-(4-((2-ethylhexyl)oxy)phenyl)-4H-dithieno[3,2-b:2',3'-d]pyrrole (M3) is presented in Scheme 1. M1 was synthesized by nucleophilic substitution that following to the procedure of previous literature.[30] M2 was synthesized by Ullmann intramolecular cyclization reaction following the previous report.[29] Then, monomer M3 was formed from M1 and M2 via Buchwald-Hartwig cross coupling reaction where $Pd(OAc)_2$, $P(t\text{-}But)_3$, NaOt-Bu were used as catalyst and ligand, respectively. In the ^{1} H NMR spectrum of monomer M3 (see Fig. S1, support information), the peaks at 7.04 ppm and 7.47 ppm are assigned for protons of "α" and "β" of thiophene ring, while those at 7.08 ppm and 7.14 ppm correspond to the protons of benzene ring linked with thiophene via C-N linker. The peaks at 3.89 ppm and peaks from 0.8 ppm to 1.8 ppm are attributed to the alkyl chains of monomer M3. In addition, the integration of the peaks indicates that 4-(4-((2-ethylhexyl)oxy)phenyl)-4H-dithieno[3,2-b:2',3'-d]pyrrole (M3) was synthesized successfully.

View Article Online
DOI: 10.1039/D0NJ02616F

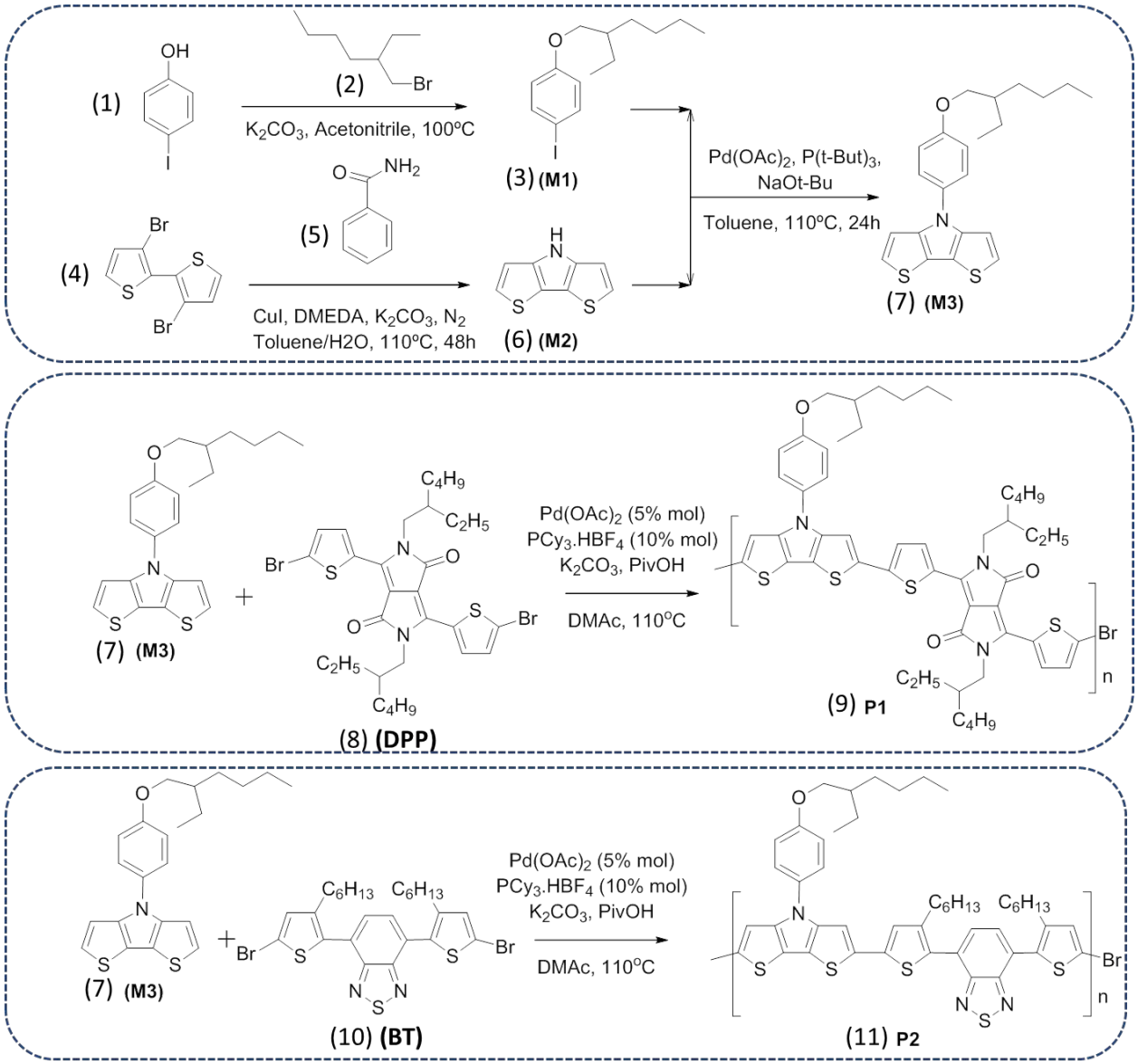

Scheme 1. Synthesis of monomers and D-A polymers P1 and P2.

The direct arylation polycondensation was carried out by Fagnou catalyst system where $Pd(OAc)_2$ was used as catalyst and PCy3.HBF_4 as ligand. The reaction was conducted in the DMAc solvent at 100 °C. At the early stage of the reaction, the color of the reaction was light yellow, and then changed to dark pink after 1 h and turned to dark blue after 24 h for the synthesis of P1. In the case of P2, the color of the reaction changed to deep orange after 1 h and turned to dark purple after 24 h. Polymers P1 and P2 were dissolved in $CHCl_3$ and filtrated via a celite layer to eliminate the Pd catalyst, and then the polymers were obtained by precipitation in cold *n*-heptane. The yields of polymerizations fluctuated between 60 and 70%. Moreover, the D-A copolymers exhibited good solubility in common organic solvents such as

View Article Online
DOI: 10.1039/D0NJ02616F

$CHCl_3$, THF, dichlorobenzene and toluene. The gel permeation chromatography (GPC) results showed that the number average molecular weights (M_n) of P1 and P2 were 12700 g mol^{-1} and 14800 g mol^{-1} with polydispersity indexes (Đ) of 1.87 and 1.65, respectively. However, the GPC traces of the polymers exhibited the unsymmetrical shape containing a shoulder in the range of low retention time, which were attributed to the high molecular weight fraction in the polymer mixture (Figure 1). It should be noted that the D-A polymers were polymerized according to the step-growth polycondensation. Therefore, couplings of oligomer/polymer segments appeared to form extremely high molecular weight fractions compared to their average molecular weights.

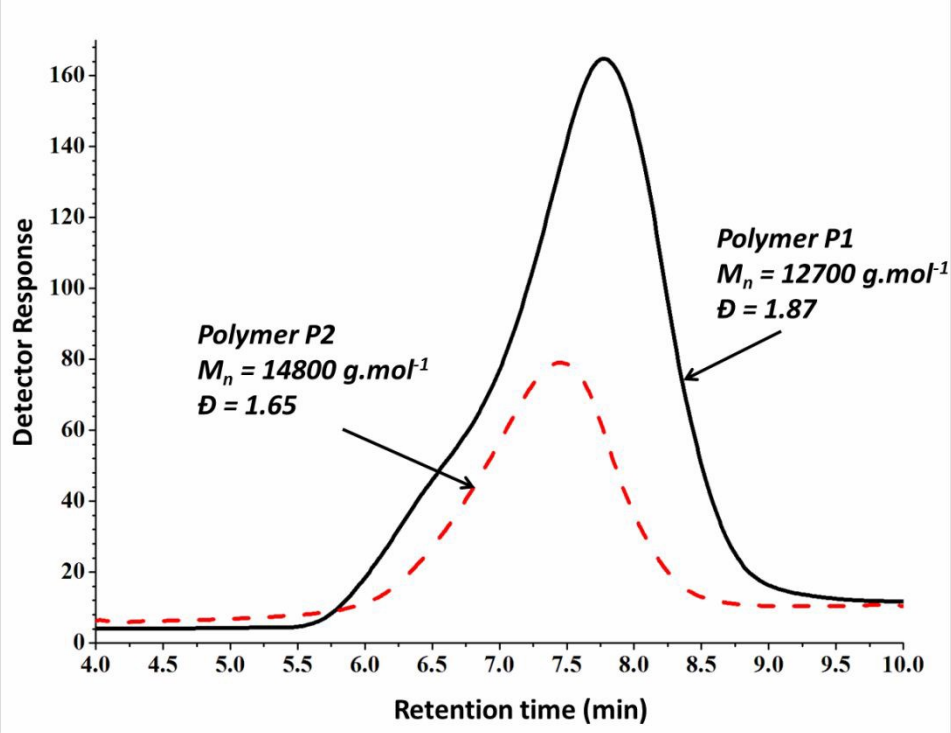

Figure 1. GPC curves of D-A conjugated polymers P1 and P2.

The vibrational properties of polymers P1 and P2 were investigated by FTIR spectroscopy (see Fig. S2). The FTIR spectra of P1 and P2 exhibited the bands from 2853 cm^{-1} to 2922 cm^{-1} attributed to the C-H stretching mode of hexyl group and C-H in aromatic structure. The band from 1585 cm^{-1} to 1492 cm^{-1} is ascribed to the aromatic C=C stretching and C-H deformation vibrations.[31,32] The broad band between 1403 cm^{-1} and 1409 cm^{-1} is presented for the C–N stretching of pyrrole moieties. In addition, the characteristic band at 1658 cm^{-1} indicates the existence of the ketone C=O group of *N*-benzoyl dithieno [3,2-b:2′,3′-d] pyrrole moiety in the structure of polymer P1. The band from 577 to 824 cm^{-1} is ascribed to the C-S stretching vibrations of thiophene structures.

View Article Online
DOI: 10.1039/D0NJ02616F

The structures of D-A polymers P1 and P2 were also investigated by ^{1}H NMR spectroscopy. In the ^{1}H NMR spectrum of P1 (Figure 2A), the peaks from 0.80 to 1.90 ppm are attributed to the alkyl side chain of P1. The peak at 4.0 ppm corresponds to the methylene protons of alkyl side chain (peak "d", Figure 2A). The multi-peaks from 6.5 ppm to 7.5 ppm (peaks "a", "b", "f" and "g") correspond to the protons in thiophene, 4H-dithieno[3,2-b:2′,3′-d]pyrrole and pyrrole aromatic structures. In addition, the broad peak at 8.98 ppm (peak "c") is assigned as a characteristic peak of thiophene units. In the ^{1}H NMR spectrum of P2 (Figure 2B), the peaks from 0.80 ppm to 1.90 ppm are also ascribed to the alkyl side chains. The peaks at 2.69 ppm and 8.07 ppm correspond to the hexyl methylene protons, which is well-known for the 3-hexylthiophene unit. The peak at 4.0 ppm (peak "a") is assigned to the methylene protons of the branched alkyl chain of M3 moieties. The peaks from 6.90 ppm to 8.07 ppm (peak "b", "c", "e", "f", and "g") are characteristic for the protons in thiophene, 4H-dithieno[3,2-b:2′,3′-d]pyrrole and benzo[c][1,2,5]thiadiazole. Based on the GPC, FTIR and ^{1}H NMR results, it can be demonstrated that D-A polymers P1 and P2 were obtained through direct heteroarylation polymerization. These polymers were also characterized via ^{13}C NMR spectroscopy. However, the results did not support clearly the determination of formation of polymers.

View Article Online
DOI: 10.1039/D0NJ02616F

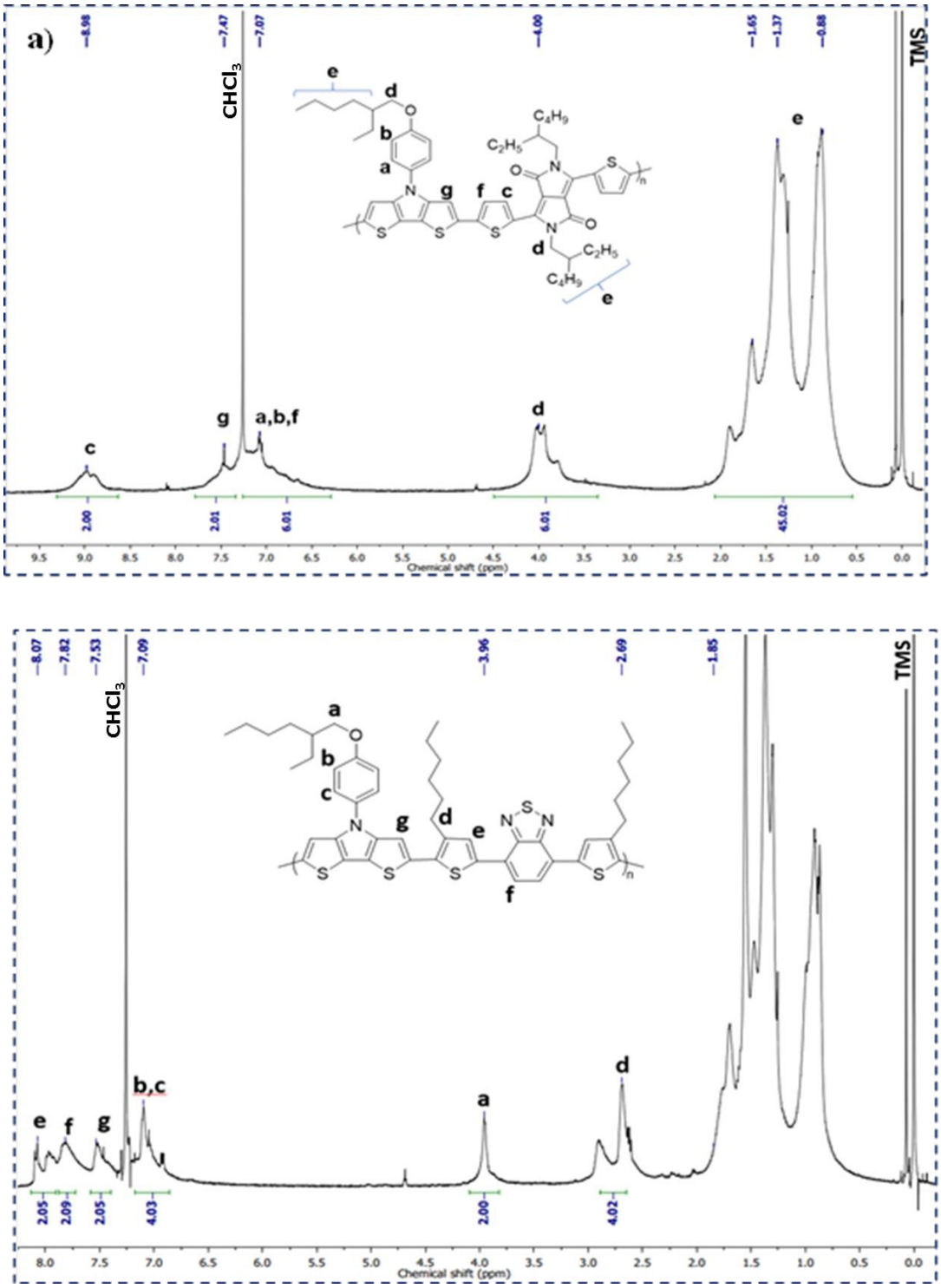

Figure 2. ^{1}HNMR spectra of P1 (a) and P2 (b) in $CDCl_3$.

View Article Online
DOI: 10.1039/D0NJ02616F

3.2 Optical and electrochemical properties of conjugated polymers

The absorption properties of polymers P1 and P2 were investigated through UV-Vis absorption spectroscopy, which was performed in dilute $CHCl_3$ solution (*ca.* 10^{-6} mol L^{-1}) and in solid state films. Polymer P2 showed an absorption maximum at 550 nm, whereas polymer P1 showed a strong red shift absorption maximum at 730 nm, which is 180 nm higher than for P2. This observation can be explained by that normally the DPP unit has an absorption maximum above 650 nm. Thus, incorporation of DPP moieties in the D-A polymer structure led to a strong red shift in absorption. In addition, the main reason causing the absorption red shift of P1 is the strong intermolecular $\pi - \pi$ stacking interactions between conjugated main chains, which enhances rigidity in its structure. Figure 3(b) presents the optical absorption spectra based on the solution-cast thin films of P1 and P2. The polymer P1 and P2 thin films exhibited absorption maxima at 800 nm and 680 nm, respectively. This phenomenon indicates again the strong intermolecular π–π stacking interactions of P1 in comparison with P2. Moreover, the λ_{onset} values of P1 and P2 were determined to be about 959 nm and 800 nm, corresponding to optical band gaps (E_g^{opt}) of 1.31 eV and 1.55 eV, respectively. Furthermore, the molar extinction coefficients (ε) of P1 and P2 were 1.2 x 10^{-4} and 1.5 x 10^{-4}, respectively. The parameters of optical properties of D-A polymers are summarized in Table 1.

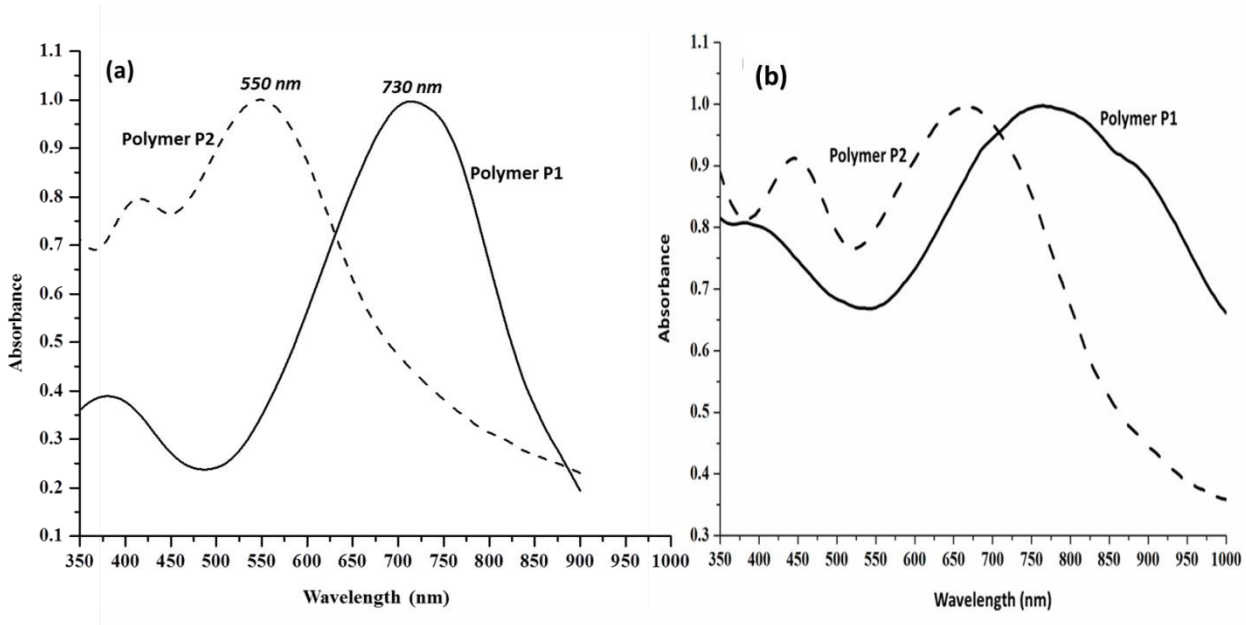

Figure 3. Absorption spectra of polymers P1 and P2 in $CHCl_3$ (a) and in solid state films (b).

To investigate the photoluminescence (PL) of P1 and P2, the PL spectra of P1 and P2 were measured in different solvents as shown in Figure 4. In $CHCl_3$ and THF (*ca.* 10^{-3} mol L^{-1}), P1 displayed

View Article Online
DOI: 10.1039/D0NJ02616F

an emission peak at 712 nm upon excitation at 450 nm, whereas P2 exhibited an emission peak at 735 nm upon excitation at 450 nm. The fluorescence quantum yields (ϕ_F) of D-A polymers in dilute $CHCl_3$ were analyzed in comparison to 9,10-diphenylanthracene as a standard (ϕ_F = 0.9). The ϕ_F of P1 and P2 showed the same value of 0.43, likely indicating the strong π –π stacking effect in both polymer structures.[33] The PL data are presented in Table 1.

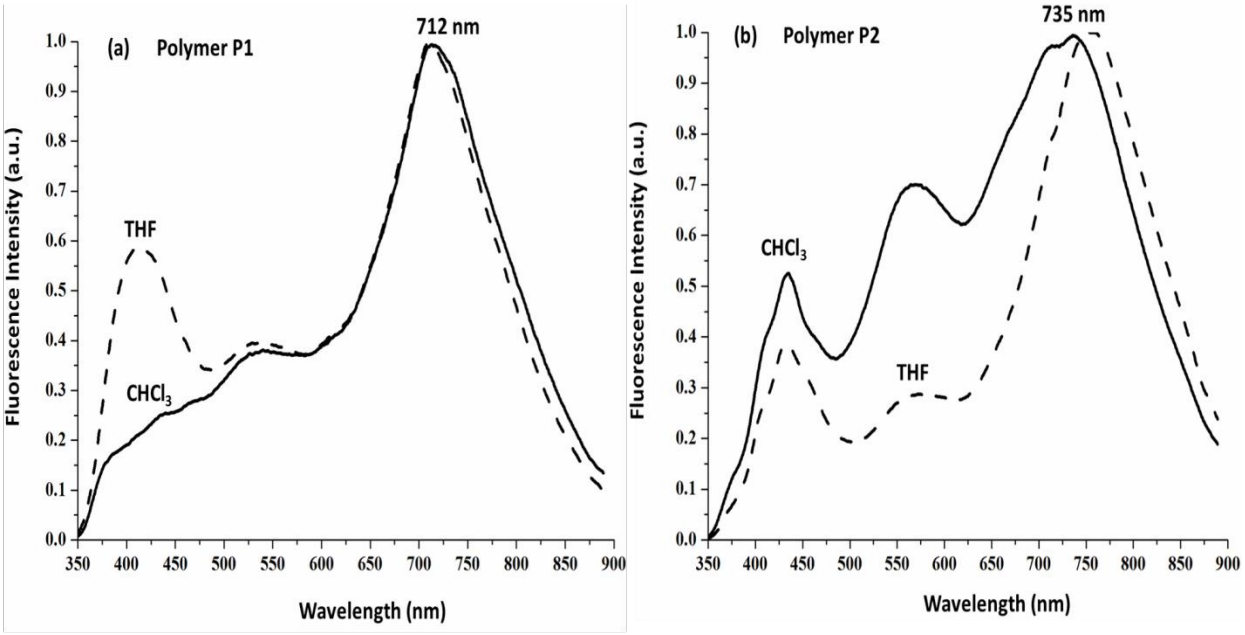

Figure 4. Fluorescence spectra of polymers P1 and P2 in $CHCl_3$ (concentrations of 10^{-3}).

Table 1. UV–vis absorption and fluorescence emission maximum wavelength, and the fluorescence quantum yields (ϕ_F) of polymer P1 and P2.

D-A Polymers	Solvent ($CHCl_3$)			Film	Optical	Molar
	UV (λ_{max}) (nm)	PL (nm)	φ_F	UV (λ_{max}) (nm)	bandgap (E_{opt}) (eV)[c]	extinction coefficient (ε)
P1	730	712	0.43	790	1.31	1.2 x 10^4
P2	550	735	0.43	670	1.55	1.5 x 10^4

The LUMO energy levels of the D-A polymers were determined from the optical band gaps which were calculated from onset absorption, while the HOMO energy levels are possibly estimated from cyclic voltammetry. Measurements of cyclic voltammetry for polymer P1 and P2 were calibrated against

View Article Online
DOI: 10.1039/D0NJ02616F

ferrocene, as an internal standard, of which ionization potential value is -4.8 eV for ferrocene/ferrocenium (Fc/Fc^+) redox system. The cyclic voltammetry curves and energy level diagrams of the D-A polymers are presented in Figure 5. The oxidation onset potentials of P1 and P2 were 0.8 and 1.1 eV, corresponding to the HOMO energy levels of -5.2 eV and -5.5 eV, respectively. The LUMO energy levels of P1 and P2 calculated from the values of the optical band gaps and HOMO energy levels were -3.89 and -3.95 eV, respectively. It is very clear that the LUMO levels of P1 and P2 are close to that of PCBM acceptor, suggesting that the polymers are useful for preparation of photovoltaic cells.

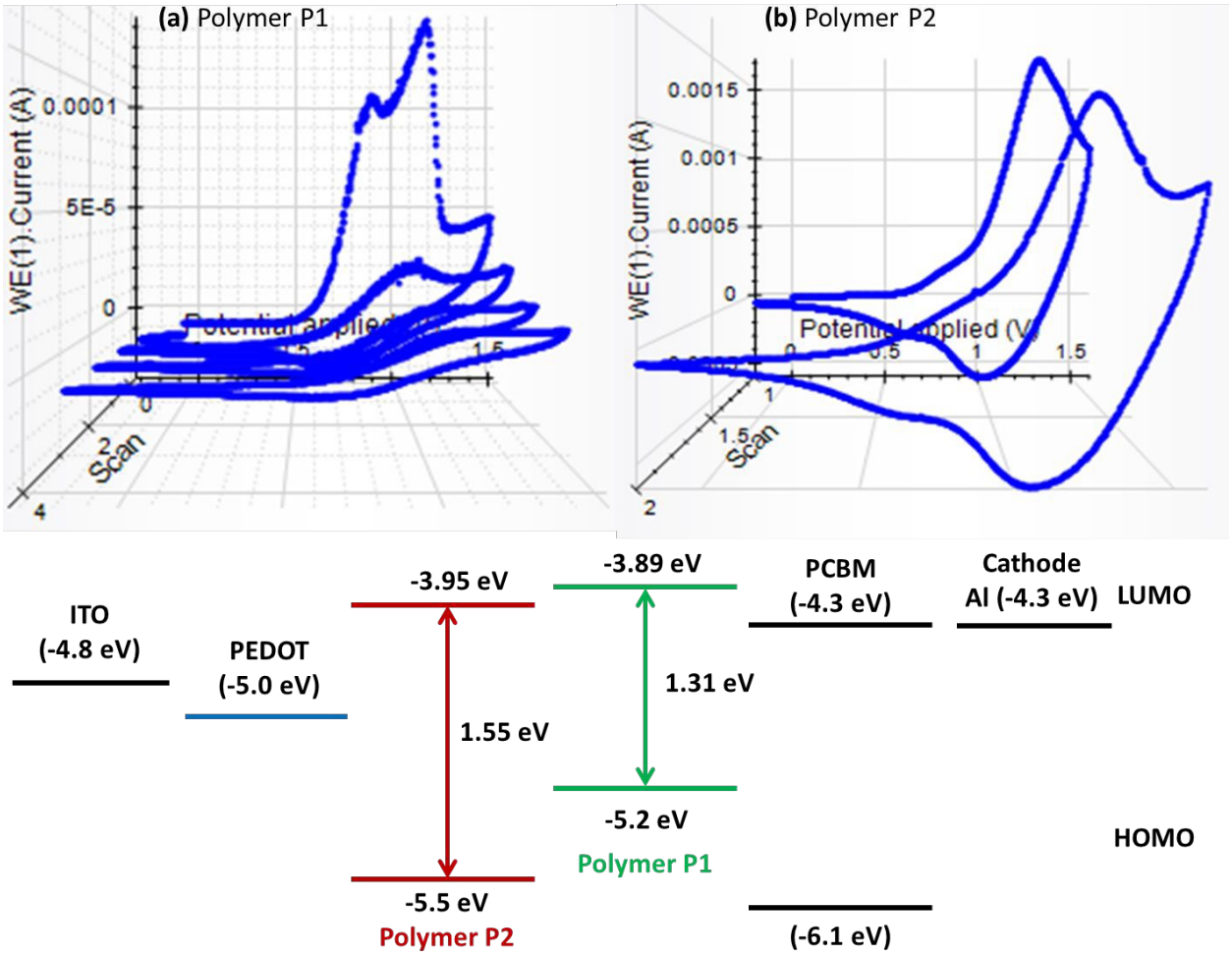

Figure 5. Cyclic voltammograms and energy diagrams of polymer P1 and P2.

3.3. Thermal and solid state properties of conjugated polymers

The thermal properties of polymers P1 and P2 were characterized by TGA and DSC. TGA analysis was performed under nitrogen flow to determine the stability of these D-A polymers in the range from room temperature to 950 °C. The polymer P2 exhibited a good thermal stability with a decomposition temperature (5% weight loss) above 350 °C, whereas polymer P1 showed a lower thermal stability with a decomposition temperature (5% weight loss) around 250 °C (see Figure 6(a)). The second

View Article Online
DOI: 10.1039/D0NJ02616F

heating run DSC diagrams in range from room temperature to 300 °C of the D-A polymers are presented in Figure 6(b). No melting transition in this temperature range was detected for both P1 and P2. Normally, the main chain of conjugated polymers is very stiff due to their strong intermolecular π–π stacking interaction, which results in high melting temperatures above 200 °C.[34-36]

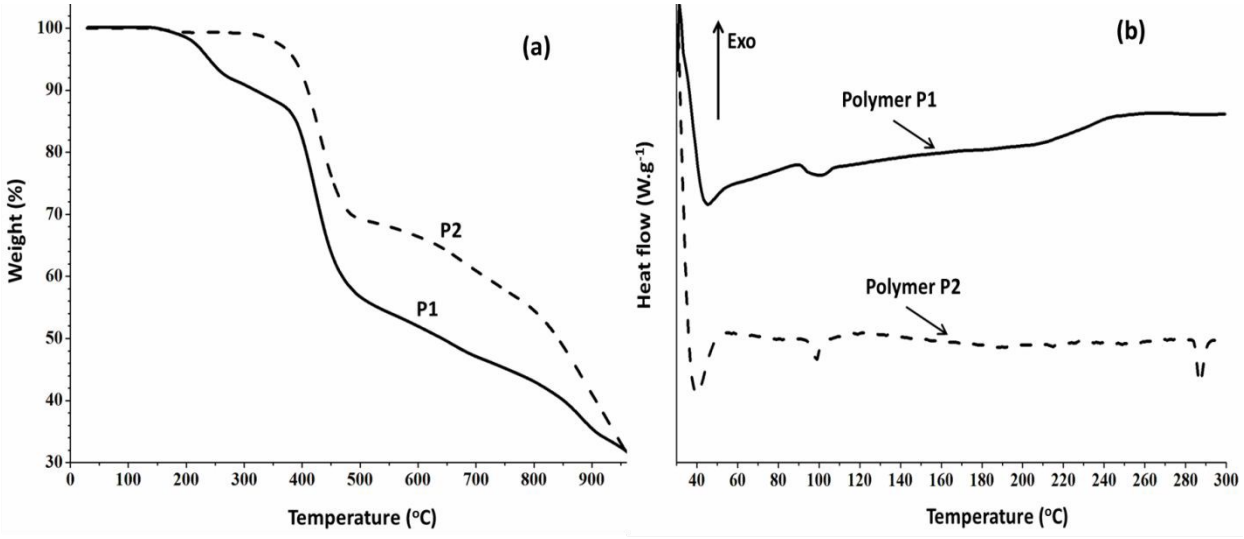

Figure 6. The TGA (a) and DSC (b) diagrams of polymers P1 and P2.

The molecular ordering of these D-A conjugated polymers in the solid state was characterized through powder XRD measurements (Figure 7). Polymer P1 exhibited several distinctive crystalline diffractions at $2\theta = 18^{o}$ (4.9 Å), 28^{o} (3.2 Å) and 40^{o} (2.3 Å), which closely correspond to the conjugated main chain distance, π–π stacking spacing and the distance between highly stacked hetero-aromatic rings, repectively,[37-38] while the broad halo centered at 23° is likely attributed to side chain disorder. On the other hand, for polymer P2, the XRD pattern showed two broad diffractions at ca. 23 and 39^{o} and diffractions associated to strong stacking orientation seem absent (or maybe overlaid by the amorphous scattering halo). This suggests that P2 more weakly aggregates than P1.

View Article Online
DOI: 10.1039/D0NJ02616F

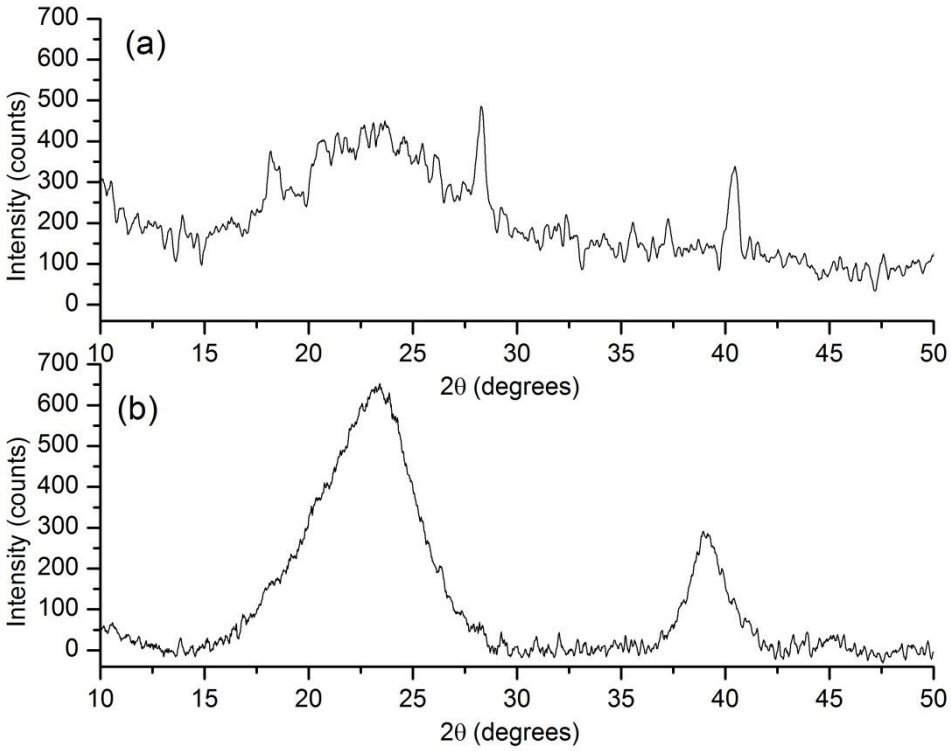

Figure 7. XRD patterns of polymer P1 (a) and P2 (b).

The microscopic and nanoscopic morphologies of thin films of D-A polymers were checked by AFM in tapping contact mode. The drop-casting technique was applied to prepare thin films onto the wafer substrates from a good solvent. Figure 8 shows the AFM images of polymers P1 and P2 after solvent annealing at 150 ^{o}C. The results revealed that the surface of polymer P1 was smoother than that of P2. The roughness value of P1 was determined 0.49 whereas P2 exhibited a roughness value of 2.11.

View Article Online
DOI: 10.1039/D0NJ02616F

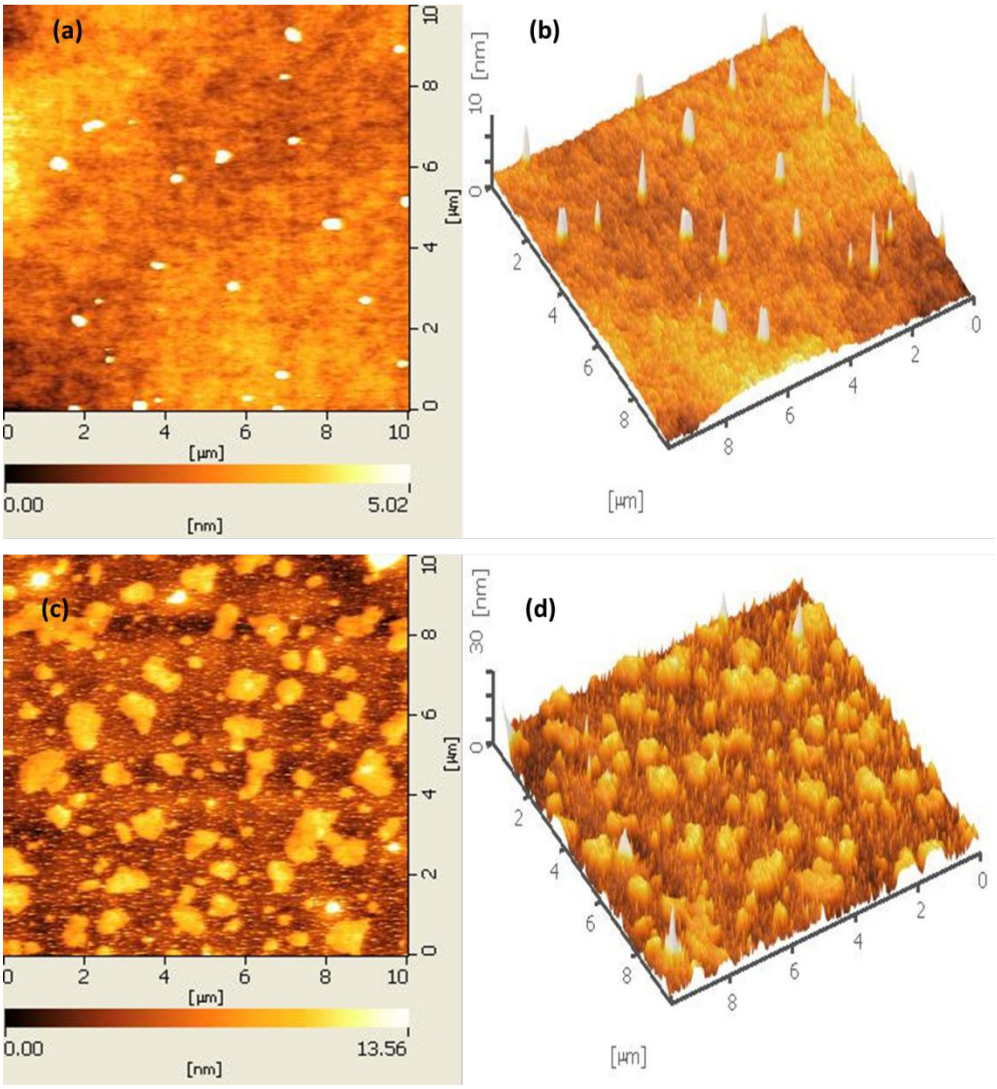

Figure 8. AFM images of D-A polymer P1 (a, 2D dimension) (b, 3D dimension) and polymer P2 (c, 2D dimension) (d, 3D dimension).

The polymers P1 and were further applied to fabricate the OFETs on oxidized silicon wafer to determine the charge mobilities of semiconducting polymers.

View Article Online
DOI: 10.1039/D0NJ02616F

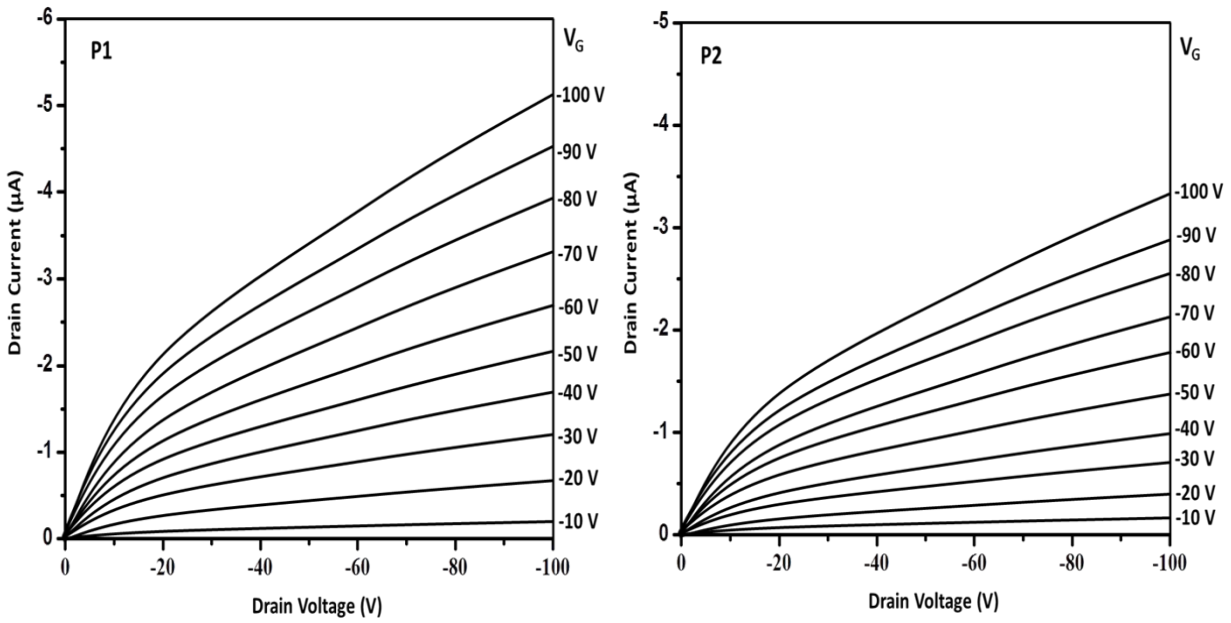

Figure 9. Drain current (I_D) versus drain voltage (V_{DS}) characteristics at different gate voltage for OFET of (A) P2 and (B) P1.

Thin film transistors based on P1 and P2 conjugated polymers exhibited typical *p*-channel output characteristics due to plot of drain current I_D vs. drain voltage at different gate voltage (V_G) (Figure 9). The mobilities of OFETs devices have been calculated according to the linear regime theory at low drain voltage following equation (1)[39,40]

$$I_{DS} = (\frac{W}{L})\mu_h C_i(V_G - V_T - V_D/2)V_D \quad \textbf{(1)}$$

Where μ_h is the field-effect mobility of holes, W is the channel width, L is the channel length, the channel length and width of the transistor are 10 μm and 700 μm respectively. The C_i is the capacitance per unit area of the gate dielectric layer (SiO_2, 300 nm. C_i = 11 nF/cm^2). V_G, V_T and V_D are gate, threshold and drain voltages, respectively. The thin film transistors based on P1 and P2 conjugated polymers exhibited hole mobilities of 1.98 x 10^{-2} cm^2/Vs and 9.54 x 10^{-3} cm^2/Vs with an on/off ratio about 10^5 and 10^3, respectively. This result suggested that the synthesized conjugated polymers are promising for organic solar cell application.

View Article Online
DOI: 10.1039/D0NJ02616F

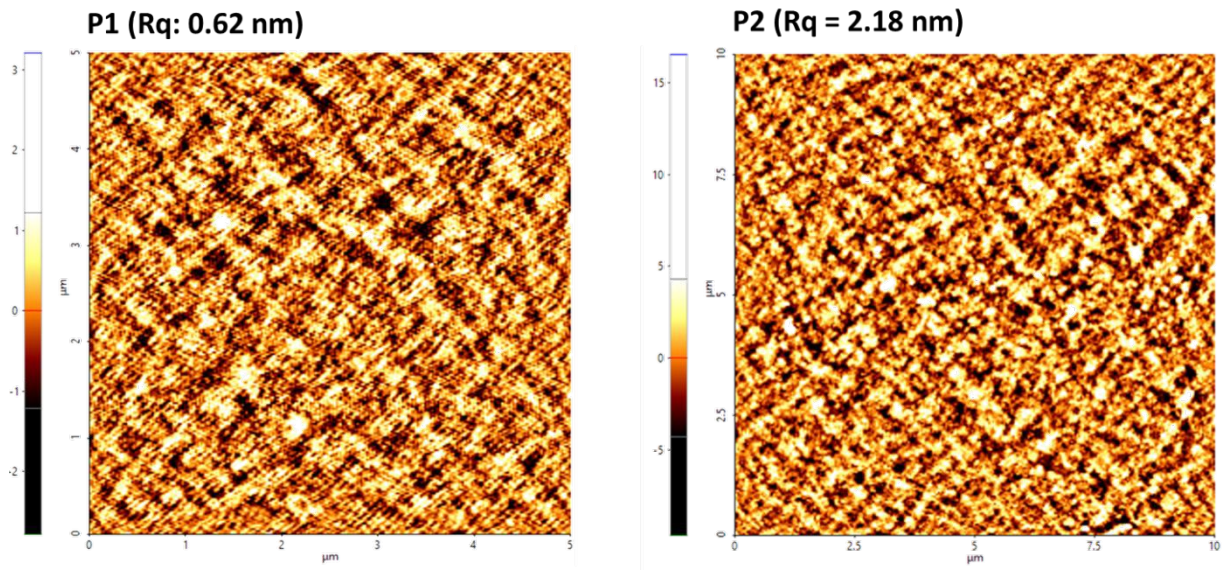

Figure 10. AFM height images (5 x 5 µm) of the blended films: (a) P1:$PC_{61}BM$ (1:1.5 w/w) and (b) P2:$PC_{61}BM$ (1:1.5 w/w).

As shown in Figure 10, the AFM images of the P2:$PC_{61}BM$ blended film showed a rough surface, with an RMS of 2.18 nm, which inhibited charge migration and exciton diffusion. In contrast, the AFM image of the P1 and PC_{61} BM blended film shows much finer domains, with an RMS of 0.62 nm, which resulted in a much higher fill factor.

3.4 Organic solar cell device fabrication

Bulk heterojunction (BHJ) polymer solar cells were fabricated following the conventional structure ITO/PEDOT:PSS/conjugated polymer:$PC_{61}BM$/Ca/Al.[41] The J_{sc}, *Voc,* fill factor (*FF*) and PCE values of the OSCs based on a BHJ structure of polymer P1 and polymer P2 are presented in Table 2. The OSCs based on P1 and P2 exhibited the same V_{oc} of 0.79 V. This suggested that the V_{oc} of OSCs is not completely reflected by the HOMO level of conjugated polymers, since the V_{oc} of cells much depends on the interaction of the electrode and activated layers as well as the parameters of cell fabrication process. The bilayer structure solar cells based on P1 and P2 showed an average PCE of 4.85% and 3.99%, respectively. The current density–voltage (*J–V)* curves of the polymer solar cell devices recorded under AM 1.5 illumination with an intensity of 100mW.cm^{-2} are plotted in Figure 11A. The EQE spectra of these devices exhibited a pronounced contribution to photocurrent generation in the wavelength range of 400-850 nm (Figure 11B). This implies that the transport of generated charges from the P1(P2)/$PC_{61}BM$ interface to the anode layer via the $PC_{61}BM$ electron channels was quite effective, which contributes to the relatively good device performance. On the other hand, the device fabricated from P1 reveals better

View Article Online
DOI: 10.1039/D0NJ02616F

EQE values than from P2. This might be attributed to either less effective contact interface between P2 and $PC_{61}BM$ or to less efficient charge transport in polymer P2. It should be noted that the PCE depends on not only the bandgap but also on the charge-carrier mobility. Therefore, the photovoltaic parameters of the BHJ solar cells fabricated from polymer P1 with $PC_{61}BM$ acceptor compound revealed that the PCE of P1 (4.85%) was much better than that of polymer P2 (3.99%) as a result of the lower bandgap energy level and higher ordering structure of P1 giving rise to more efficient charge transport.

Table 2. Photovoltaic parameters of OSCs based on polymer P1 and polymer P2 using $PC_{61}BM$ as acceptor counterpart in optimized ratios under the illumination of AM 1.5G, 100 $mW.cm^{-2}$.

D-A Polymer/Fullerene	V_{oc} (V)	J_{sc} (mA/cm^2)	FF (%)	PCE (Avg.) %
P1/$PC_{61}BM$	0.79	12.82	47.98	4.85
P2/$PC_{61}BM$	0.79	13.24	38.24	3.99

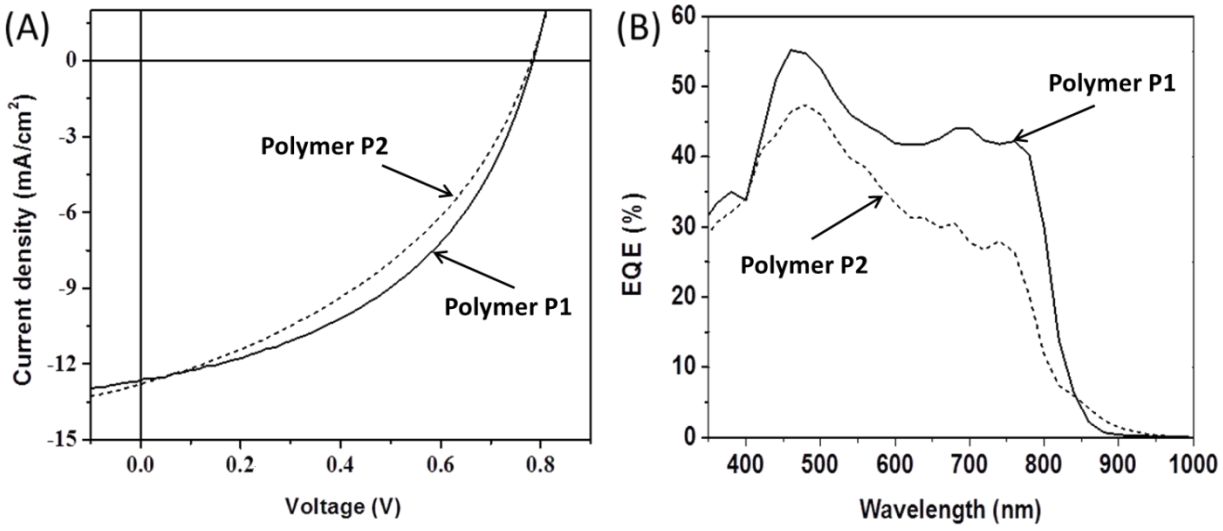

Figure 11. Current–voltage characteristics of the bulk heterojunction polymeric solar cells prepared from polymers P1 and P2 as donor polymer, and $PC_{61}BM$ fullerene acceptor (A) and EQE spectra of solar cells based on P1 and P2 (B).

4. Conclusion

In conclusion, newly designed D-A conjugated polymers based on 4-(4-((2-ethylhexyl)oxy)phenyl)-4H-dithieno[3,2-b:2',3'-d]pyrrole (EPDP) and 3,6-bis(5-bromothiophen-2-yl)-2,5-

View Article Online
DOI: 10.1039/D0NJ02616F

bis(2-ethylhexyl)-2,5-dihydropyrrolo[3,4-c]pyrrole-1,4-dione (BTBP) or 4,7-bis(5-bromothiophen-2-yl)benzo[c][1,2,5]thiadiazole (BT) units were synthesized successfully in 65-69% yields through direct(hetero)arylation polymerization. The D-A polymers P1 and P2 were characterized, exhibiting low bandgap energy levels of 1.31 eV and 1.55 eV, respectively. Both polymers P1 and P2 were used to fabricate BHJ organic solar cells in combination with $PC_{61}BM$ with PCEs of 4.85% and 3.99%, respectively. This work demonstrated the potential of new D-A conjugated polymers for achieve efficient organic photovoltaic devices.

Conflicts of interest

The authors declare no competing financial interest.

Acknowledgements

This research was fully supported by the Vietnam National Foundation for Science and Technology Development (NAFOSTED) under grant number "104.02-2017.339"

References

1. H.-Y. Chen, M. Nikolka, A. Wadsworth, W. Yue, A. Onwubiko, M. Xiao, A. J. P. White, D. Baran, H. Sirringhaus and I. McCulloch, *Macromolecules*, 2018, **51**, 71-79.
2. C. Guo, Y.-H. Lin, M. D. Witman, K. A. Smith, C. Wang, A. Hexemer, J. Strzalka, E. D. Gomez and R. Verduzco, *Na. Lett*, 2013, **13**, 2957-2963.
3. Y. Bai, J. Zhang, D. Zhou, Y. Wang, M. Zhang and P. Wang, *J. Am. Chem. Soc.*, 2011, **133**, 11442-11445.
4. S. Bi, Y. Li, Z. He, Z. Ouyang, Q. Guo and C. Jiang, *Org. Electron.*, 2019, **65**, 96-99.
5. P. Cheng, G. Li, X. Zhan and Y. Yang, *Nat. Phot.*, 2018, **12**, 131-142.
6. V. Tamilavan, M. Song, S. Kim, R. Agneeswari, J.-W. Kang and M. H. Hyun, *Polymer*, 2013, **54**, 3198-3205.
7. H. Kim, S. Nam, J. Jeong, S. Lee, J. Seo, H. Han and Y. Kim, *K. J. Chem. Eng.*, 2014, **31**, 1095-1104.
8. C. C. Chen, W. H. Chang, K. Yoshimura, K. Ohya, J. You, J. Gao, Z. Hong and Y. Yang, *Adv. Mater.*, 2014, **26**, 5670-5677.
9. A. R. bin Mohd Yusoff, D. Kim, H. P. Kim, F. K. Shneider, W. J. da Silva and J. Jang, *Ener. Env. Sci.*, 2015, **8**, 303-316.
10. W. Li, K. H. Hendriks, A. Furlan, M. M. Wienk and R. A. Janssen, *J. Am. Chem. Soc.*, 2015, **137**, 2231-2234.
11. J. D. Chen, C. Cui, Y. Q. Li, L. Zhou, Q. D. Ou, C. Li, Y. Li and J. X. Tang, *Adv. Mater.*, 2015, **27**, 1035-1041.
12. T. Earmme, Y.-J. Hwang, N. M. Murari, S. Subramaniyan and S. A. Jenekhe, *J. Am. Chem. Soc.*, 2013, **135**, 14960-14963.
13. H. Li, T. Earmme, S. Subramaniyan and S. A. Jenekhe, *Adv. Ener. Mater.*, 2015, **5**, 1402041.
14. M. T. Dang, L. Hirsch, G. Wantz and J. D. Wuest, *Chem. Rev.*, 2013, **113**, 3734-3765.
15. H. Li, Y. J. Hwang, B. A. Courtright, F. N. Eberle, S. Subramaniyan and S. A. Jenekhe, *Adv. Mater.*, 2015, **27**, 3266-3272.
16. Y. Lin, Y. Li and X. Zhan, *Chem. Soc. Rev.*, 2012, **41**, 4245-4272.

View Article Online
DOI: 10.1039/D0NJ02616F

17. Q. Liu, Y. Jiang, K. Jin, J. Qin, J. Xu, W. Li, J. Xiong, J. Liu, Z. Xiao, K. Sun, S. Yang, X. Zhang and L. Ding, *Science Bulletin., 2020,* ***65,*** 272-275.
18. K. H. Hendriks, W. Li, M. M. Wienk and R. A. Janssen, *J. Am. Chem. Soc.*, 2014, **136**, 12130-12136.
19. X. Zhang, T. T. Steckler, R. R. Dasari, S. Ohira, W. J. Potscavage, S. P. Tiwari, S. Coppée, S. Ellinger, S. Barlow and J.-L. Brédas, *J. Mater. Chem.*, 2010, **20**, 123-134.
20. L. Hu, W. Qiao, X. Zhou, J. Han, X. Zhang, D. Ma, Y. Li and Z. Y. Wang, *Polym. Chem.*, 2017, **8**, 2055-2062.
21. L. Dou, W. H. Chang, J. Gao, C. C. Chen, J. You and Y. Yang, *Adv. Mater.*, 2013, **25**, 825-831.
22. R. S. Ashraf, I. Meager, M. Nikolka, M. Kirkus, M. Planells, B. C. Schroeder, S. Holliday, M. Hurhangee, C. B. Nielsen and H. Sirringhaus, *J. Am. Chem. Soc.*, 2015, **137**, 1314-1321.
23. H. Choi, S. J. Ko, T. Kim, P. O. Morin, B. Walker, B. H. Lee, M. Leclerc, J. Y. Kim and A. J. Heeger, *Adv. Mater.*, 2015, **27**, 3318-3324.
24. H. Zhou, L. Yang, A. C. Stuart, S. C. Price, S. Liu and W. You, *Angewandte Chemie International Edition*, 2011, **50**, 2995-2998.
25. Y. Chen, Q. Zhang, M. Du, G. Li, Z. Li, H. Huang, Y. Geng, X. Zhang and E. Zhou, *ACS App. Poly. Mater.*, 2019, **1**, 906-913.
26. Y. Geng, J. Cong, K. Tajima, Q. Zeng and E. Zhou, *Poly. Chem.*, 2014, **5**, 6797-6803.
27. P. Nagarjuna, A. Bagui, V. Gupta and S. P. Singh, *Org. Electron.*, 2017, **43**, 262-267.
28. Q. Wan , X. Guo , Z. Wang , W. Li , B. Guo , W. Ma , M. Zhang and Y. Li, *Adv. Funct. Mater.*, 2016, **26**, 6635–6640
29. S. Kowalski, S. Allard, K. Zilberberg, T. Riedl and U. Scherf, *Prog. Poly. Sci*, 2013, **38**, 1805-1814.
30. A. Facchetti, L. Vaccaro and A. Marrocchi, *Angewandte Chemie International Edition*, 2012, **51**, 3520-3523.
31. J. Coates, Interpretation of infrared spectra, a practical approach, in Encyclopedia of Analytical Chemistry, ed. By Meyers R. A and McKelvy M. L. Wiley Online Library, 2006.
32. S. Schmid S, J. Gacanin, Y. Wu, T. Weil and P. Bäuerle, *Polym Chem.*, 2017, 8, 7113–7118.
33. C. Kanimozhi, N. Yaacobi-Gross, E. K. Burnett, A.L. Briseno, T. D. Anthopoulos and U. Salzneret., *Phys Chem Chem Phys*, 2014, **16**, 17253–17265.
34. A. Zen, M. Saphiannikova, D. Neher, J. Grenzer, S. Grigorian and U. Pietsch U., *Macromolecules,*2006*,* **39**, 2162–2171.
35. G. Koeckelberghs, L. D. Cremer, A. Persoons and T. Verbiest, *Macromolecules,* 2007*,* **40**, 4173–4181.
36. W. Zhang, J. Li , L. Zou, B. Zhang, J. Qin and Z. Lu Z., *Macromolecules*, 2008, **41**, 8953–8955.
37. Y. Yuan, J. Zhang, J. Sun, J. Hu, T. Zhang and Y. Duan Y., *Macromolecules*, 2011, **44**, 9341–9350.
38. S. Dag and L. W. Wang, *J Phys Chem B* , 2010, **114**, 5997–6000.
39. Horowitz G., *Adv Mater*. 1998, **10**, 365-377
40. M. Urien, G. Wantz, E. Cloutet, L. Hirsch, P. Tardy, L. Vignau, H. Cramail and J. P. Parneix., *Org Electron*, 2007, **8**, 727-734.
41. L. T. P. Boudreault, A. Najari and M. Leclerc M., *Chem Mater, 2011,* **23**, 456–469.

View Article Online
DOI: 10.1039/D0NJ02616F

View Article Online
DOI: 10.1039/D0NJ02616F

Synthesis and Characterization of Donor-Acceptor Semiconducting Polymers Containing 4-(4-((2-ethylhexyl)oxy)phenyl)-4H-dithieno[3,2-b:2',3'-d]pyrrole for Organic Solar Cells

Huyen Le Thi Mai[1], Nhung Thanh Thi Truong[1], Thiet Quoc Nguyen[4], Bao Kim Doan[1], Dat Hung Tran[1], Le-Thu T.Nguyen[2], Lee Woosung[3], Jae Woong Jung[5], Mai Ha Hoang[6], Ha Phuong Ky Huynh[1], Chau Duc Tran[2], Ha Tran Nguyen*[1,2]*

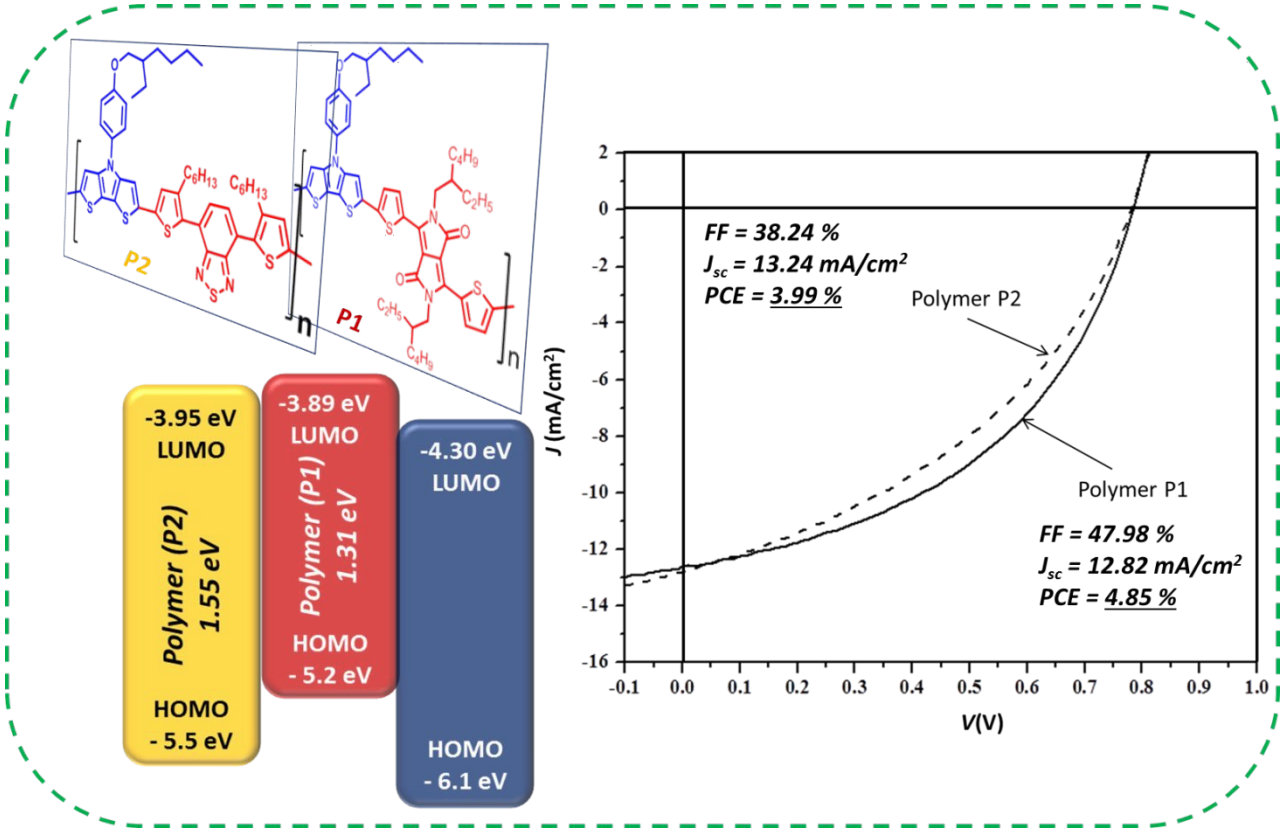

The novel donor–acceptor conjugated polymers containing 4-(4-((2-ethylhexyl)oxy)phenyl)-4H-dithieno[3,2-b:2',3'-d]pyrrole and 2,5-bis(2-ethylhexyl)-3,6-di(thiophen-2-yl)pyrrolo[3,4-c]pyrrole-1,4(2H,5H)-dione were successfully synthesized via direct arylation polymerization. The obtained donor–acceptor conjugated polymers have been applied for the organic solar cells which exhibited the PCE of 4.85%.